Time-Domain Passivity Control of Haptic Interfaces

Blake Hannaford, *Senior Member, IEEE*, and Jee-Hwan Ryu

***Abstract*—A patent-pending, energy-based method is presented for controlling a haptic interface system to ensure stable contact under a wide variety of operating conditions. System stability is analyzed in terms of the time-domain definition of passivity. We define a "Passivity Observer" (PO) which measures energy flow in and out of one or more subsystems in real-time software. Active behavior is indicated by a negative value of the PO at any time. We also define the "Passivity Controller" (PC), an adaptive dissipative element which, at each time sample, absorbs exactly the net energy output (if any) measured by the PO. The method is tested with simulation and implementation in the Excalibur haptic interface system. Totally stable operation was achieved under conditions such as stiffness $>$100 N/mm or time delays of 15 ms. The PO/PC method requires very little additional computation and does not require a dynamical model to be identified.**

***Index Terms*—Haptic interface, passivity controller, passivity observer, time-domain passivity.**

I. INTRODUCTION

ONE OF the most significant problems in haptic interface design is to create a control system which simultaneously is stable (i.e., does not exhibit vibration or divergent behavior) and gives high fidelity under any operating conditions and for any virtual environment parameters. A classic engineering tradeoff is presented since realism of the haptic interface (for example, in terms of stiffness of "hard" objects) must often be reduced in order to guarantee totally stable operation. Initial efforts to solve this problem introduced the "virtual coupling" between the virtual environment and the haptic device [1], [2]. The virtual coupling is a virtual mechanical system containing a combination of series and parallel elements interposed between the haptic interface and the virtual environment to limit the maximum or minimum impedance presented by the virtual environment in such a way as to guarantee stability. Particulars of virtual coupling design depend the causality of the virtual environment (VE) and the haptic device. By causality, we refer to the selection of velocity or force as input and its complement (force or velocity) as output. Possible VE causalities include impedance-based (position/velocity input, force output), admittance-based (force input, position/velocity output), or constraint based (position input/position output). In the case of an impedance-based environment (typical of many implemented systems), a virtual spring and damper in parallel are typically connected in series between the haptic interface and the virtual environment. Stability in this case depends inversely on the stiffness being rendered by the system and the series stiffness has the effect of setting the maximum stiffness. Correct selection of the virtual coupling parameters will allow the highest possible stiffness without introducing instability.

The virtual coupling parameters can be set empirically, but several previous research projects have sought out a theoretical design procedure.

Interesting VEs are always nonlinear and the dynamic properties of a human operator are always involved. These factors make it difficult to analyze haptic systems in terms of known parameters and linear control theory. One fruitful approach is to use the idea of passivity to guarantee stable operation. Anderson and Spong [3] and Neimeyer and Slotine [4] have used passivity ideas in the related area of stable control of force-feedback teleoperation with time delay. Colgate and Schenkel [5] have used it to derive fixed parameter virtual couplings (i.e., haptic interface controllers).

Passivity is a sufficient condition for stability which has the following attractive features:

- uses intuitively attractive energy concepts: a system is passive if and only if the energy flowing in exceeds the energy flowing out for all time;
- allows a global stability conclusion to be drawn from considering system blocks individually;
- applies to linear and nonlinear systems;
- has shown through experience and some evidence [6] that it is safe to assume the human operator is passive at frequencies of interest.

The major problem with using passivity for design of haptic interaction systems is that it is too conservative. In many cases, performance can be poor if a fixed damping value is used to guarantee passivity under all operating conditions.

Haptic interfaces share with force feedback teleoperator systems the interesting property that information and energy flows in two directions through a single interface between the human operator and the virtual or real environment. This property means that ideas from the theory of electrical networks (or more generally the "general systems theory" of Paynter [7]) can be applied to good effect [8], [4]. The virtual coupling is one example of such a network.

Adams [9] derived a method of virtual coupling design from two-port network theory which applied to all causality combinations and was less conservative than passivity based design. They were able to derive optimal virtual coupling parameters using a dynamic model of the haptic device and by satisfying Lewellyn's "absolute stability criterion," an inequality composed of terms in the two-port description of the combined

Manuscript received May 31, 2001. This paper was recommended for publication by Associate Editor C. Melchiorri and Editor A. De Luca upon evaluation of the reviewers' comments. This work was supported in part by a grant from Ford Motor Company and Korea Science and Engineering Foundation.

B. Hannaford is with the Department of Electrical Engineering, University of Washington, Seattle, WA 98195-2500 USA (e-mail: blake@u.washington.edu).

J.-H. Ryu is with the Department of Mechanical Engineering, Korea Advanced Institute of Science and Technology, Taejeon 305-701, Korea (e-mail: jhryu@kaist.ac.kr).

Publisher Item Identifier S 1042-296X(02)01813-X.

haptic interface and virtual coupling system. This procedure guaranteed a stable and high-performance virtual coupling as long as the VE was passive. Miller *et al.* have derived another design procedure which extends the analysis to nonlinear environments and extracts a damping parameter to guarantee stable operation [10]–[12].

There are several mechanisms by which a VE or other part of the system might exhibit active behavior even when it is designed to be passive. These include delays due to numerical integration schemes, quantization [1] and interactions between the discrete time system, and the continuous time device/human operator [5]. These contributing factors to instability have been termed "energy leaks" by Gillespie and Cutkosky [13].

Yokokohji *et al.* [14] studied teleoperation in the presence of time delay. Their control method exhibited undesirable behavior in the case of sudden loss of the communication link. They computed an online estimate of energy production/dissipation using wave variables and used this estimate to disable system operation in the case of instability due to link loss.

In this paper, we will develop analysis and control of instability in complex systems such as haptic interfaces using the time-domain definition of passivity (see below). We define the "Passivity Observer" and the "Passivity Controller" and show how they can be applied to haptic interfaces in place of fixed-parameter virtual couplings. We then study properties of the controller through simulation and experimental evaluation in our previously described Excalibur system [15], [16].

II. Definitions

In this section, we review passivity properties of networks and define our observer and controller. First, we define the sign convention for all forces and velocities so that their product is positive when power enters the system port (Fig. 1). We also assume that the system has initial stored energy at $t = 0$ of $E(0)$.

We then use the following widely known definitions of passivity.

Definition 1: The one-port network, N, with initial energy storage $E(0)$ is passive if and only if

$$\int_0^t f(\tau)v(\tau)\,d\tau + E(0) \geq 0, \qquad \forall t \geq 0 \tag{1}$$

for admissible force (f) and velocity (v).

Equation (1) states that the energy supplied to a passive network must be greater than negative $E(0)$ for all time [9], [17], [18], [19].

Definition 2: The M-port network, N_M, with initial energy storage $E(0)$ is passive if and only if

$$\int_0^t (f_1(\tau)v_1(\tau) + \cdots + f_M(\tau)v_M(\tau))\,d\tau + E(0) \geq 0, \qquad \forall t \geq 0 \tag{2}$$

for all admissible forces $(f_1, \ldots, f_M)$ and velocities $(v_1, \ldots, v_M)$.

The elements of a typical haptic interface system include the VE, the virtual coupling network, the haptic device controller, the haptic device, and the human operator. Many of the input and output variables of these elements of haptic interface systems can be measured by the computer, and (1) and (2) can be computed in real time by appropriate software. This software is very simple in principle because, at each time step, (1) or (2) can be evaluated with few mathematical operations.

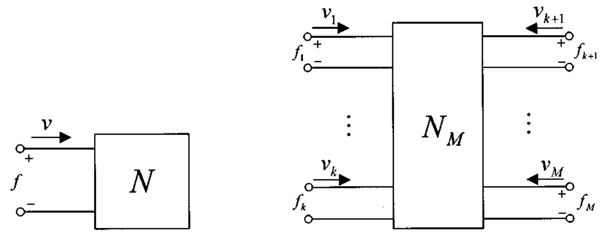

Fig. 1. One-port and M-port networks representing components of a haptic interface system.

A. Passivity Observer

The conjugate variables which define power flow in such a computer system are discrete-time values. We confine our analysis to systems having sampling rate substantially faster than the dynamics of the haptic device, human operator, and virtual environment so that the change in force and velocity with each sample is small. Many haptic interface systems (including our own, detailed in Section V) have sampling rates of 1000 Hz, more than ten times the highest significant mode in our system. Thus, we can easily "instrument" one or more blocks in the system with the following passivity observer (PO):

$$E_{\mathrm{obsv}}(n) = \Delta T \sum_{k=0}^{n} f(k)v(k) \tag{3}$$

where ΔT is the sampling period. For an M-port network with zero initial energy storage, we have

$$E_{\mathrm{obsv}}(n) = \Delta T \sum_{k=0}^{n} [f_1(k)v_1(k) + \cdots + f_M(k)v_M(k)]. \tag{4}$$

If $E_{\mathrm{obsv}}(n) \geq 0$ for every n, this means the system dissipates energy. If there is an instance that $E_{\mathrm{obsv}}(n) < 0$, this means the system generates energy and the amount of generated energy is $-E_{\mathrm{obsv}}(n)$. When there are multiple interconnected elements, we might want to observe each one separately in order to determine which ones are active and which are passive.

Example: Let us consider a network of arbitrarily connected N-port elements as shown in Fig. 2. If we define a PO for each element, and assume zero initial stored energy, we can compute the total system energy by adding that of each element

$$E_{N_1}(n) = \Delta T \sum_{k=0}^{n} [f_1(k)v_1(k) + f_2(k)v_2(k) - f_3(k)v_3(k)] \tag{5}$$

$$E_{N_2}(n) = -\Delta T \sum_{k=0}^{n} f_2(k)v_2(k) \tag{6}$$

$$E_{N_3}(n) = \Delta T \sum_{k=0}^{n} [f_3(k)v_3(k) - f_4(k)v_4(k) - f_5(k)v_5(k)] \tag{7}$$

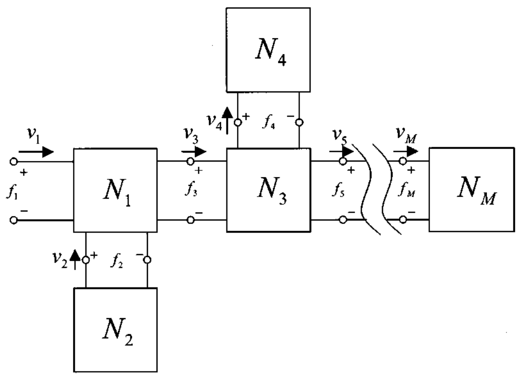

Fig. 2. Example of an arbitrarily connected network system with one open end. Each block can be either passive or active. Entire system passivity is the sum of individual blocks.

$$E_{N_4}(n) = \Delta T \sum_{k=0}^{n} f_4(k) v_4(k) \tag{8}$$

$$E_{N_M}(n) = \Delta T \sum_{k=0}^{n} f_M(k) v_M(k). \tag{9}$$

Total energy is

$$E_{\text{obsv}}(n) = E_{N_1}(n) + E_{N_2}(n) + E_{N_3}(n) + E_{N_4}(n) + \cdots + E_{N_M}(n). \tag{10}$$

The total energy determines whether or not the entire network is passive or active. If each of the individual energies is substituted into (10), we get the interesting result

$$E_{\text{obsv}}(n) = \Delta T \sum_{k=0}^{n} f_1(k) v_1(k). \tag{11}$$

In the previous example, we have left one port unconnected and the PO for the network reduced to (11), which depends only on $f_1 v_1$. There are three ways that this network can be terminated: 1) open circuit ($v_1 = 0$); 2) short circuit ($f_1 = 0$); and 3) a one-port network ($f_1 v_1 \neq 0$). In all three cases, if we add in a PO for the last element, the total energy becomes zero for all possible networks. This is a consequence of Tellegen's theorem [20]. When we have one port undefined as we have in (11), we are observing the behavior of part of a system, in particular, how much energy flows in or out.

We will refer to a port as "open-ended" when it is connected as in "3)" above, but the analysis stops at that point. We then can restate the definition of passivity in the context of a M-port system with multiple subcomponents.

Theorem 1: For any arbitrarily connected network system with P open ends, the amount of dissipated or generated energy can be calculated using input and output values of the open-ended port(s) such as

$$E_{\text{obsv}}(n) = \Delta T \sum_{k=0}^{n} [f_1(k) v_1(k) + \cdots + f_P(k) v_P(k)] \tag{12}$$

and if $E_{\text{obsv}}(n) \geq 0$ for every n, this system dissipates energy; otherwise, if there is an instance that $E_{\text{obsv}}(n) < 0$, this system generates energy and the amount of generated energy is $-E_{\text{obsv}}(n)$.

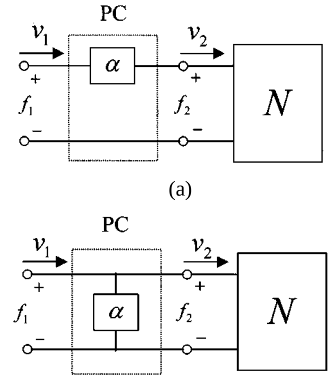

(a)

(b)

Fig. 3. (a) Series and (b) parallel configurations of PCs for one-port networks. α is an adjustable damping element. Choice of configuration depends on input/output causality of model underlying the one-port.

B. Passivity Controller

Consider a one-port system which may be active. Depending on operating conditions and the specifics of the one-port element's dynamics, the value of the PO may or may not be negative at a particular time. However, if it is negative at any time, we know that the one-port may then be contributing to instability. Moreover, we know the exact amount of energy generated and we can design a time-varying element to dissipate only the required amount of energy. We will call this element a passivity controller (PC).

The PC takes the form of a dissipative element in a series or parallel configuration (Fig. 3). Both obey the constitutive equation

$$f = \alpha v. \tag{13}$$

Specifically, for the series connection [Fig. 3(a)]

$$f_1 = f_2 + \alpha v \tag{14}$$

and for the parallel case

$$v_2 = v_1 - \frac{f_1}{\alpha}. \tag{15}$$

For a series PC with impedance causality, we compute α in real time as follows:

1) $v_1(n) = v_2(n)$ is an input.
2) $f_2(n) = F_{VE}(v_2(n))$ where $F_{VE}()$ is the output of the virtual environment.
3) $E_{\text{obsv}}(n) = E_{\text{obsv}}(n-1) + [f_2(n) v_2(n) + \alpha(n-1) v_2(n-1)^2] \Delta T$.
4)

$$\alpha(n) = \begin{cases} -E_{\text{obsv}}(n)/\Delta T v_2(n)^2, & \text{if } E_{\text{obsv}}(n) < 0 \\ 0, & E_{\text{obsv}}(n) \geq 0. \end{cases} \tag{16}$$

5) $f_1(n) = f_2(n) + \alpha(n) v_2(n) \Rightarrow$ output.

Note that ΔT can be canceled from (3) and (4) for brevity and to reduce computation. Thus, we can also express the PO as

$$W(n) = \sum_{k=0}^{n} f_2(k)v_2(k) + \sum_{k=0}^{n-1} \alpha(k)v_2(k)^2 \tag{17}$$

where

$$W(n) = \frac{1}{\Delta T} E_{\mathrm{obsv}}(n).$$

We can easily demonstrate that the system computed by (16) is passive

$$\sum_{k=0}^{n} f_1(k)v_1(k) = \sum_{k=0}^{n} f_2(k)v_2(k) + \sum_{k=0}^{n} \alpha(k)v_2(k)^2 \tag{18}$$

$$\begin{aligned}\sum_{k=0}^{n} f_1(k)v_1(k) &= \sum_{k=0}^{n} f_2(k)v_2(k) + \sum_{k=0}^{n-1} \alpha(k)v_2(k)^2 \\ &\quad + \alpha(n)v_2(n)^2 \\ &= W(n) + \alpha(n)v(n)^2\end{aligned} \tag{19}$$

using (16),

$$\sum_{k=0}^{n} f_1(k)v_1(k) \geq 0 \qquad \forall n.$$

We can similarly derive the case of admittance causality with a parallel PC.

1) $f_1(n) = f_2(n)$ is an input.
2) $v_2(n) = V_{VE}(f_2(n))$ where $V_{VE}(\,)$ is the admittance of the virtual environment.
3)

$$W(n) = W(n-1) + f_2(n)v_2(n) + \frac{1}{\alpha(n-1)} f_2(n-1)^2.$$

4)

$$\frac{1}{\alpha(n)} = \begin{cases} \dfrac{-W(n)}{f_2(n)^2}, & \text{if } W(n) < 0 \\ 0, & W(n) \geq 0. \end{cases} \tag{20}$$

5)

$$v_1(n) = v_2(n) + \frac{1}{\alpha(n)} f_2(n) \Rightarrow \text{output}.$$

We can also write the PO as

$$W(n) = \sum_{k=0}^{n} f_2(k)v_2(k) + \sum_{k=0}^{n} \frac{1}{\alpha(k)} f_2(k)^2 \tag{21}$$

which gives the following passivity proof:

$$\begin{aligned}&\sum_{k=0}^{n} f_1(k)v_1(k) \\ &\quad = \sum_{k=0}^{n} f_2(k)v_2(k) + \sum_{k=0}^{n-1} \frac{1}{\alpha(k)} f_2(k)^2 + \frac{1}{\alpha(n)} f_2(n)^2 \\ &\quad = W(n) + \frac{1}{\alpha(n)} f_2(n)^2\end{aligned} \tag{22}$$

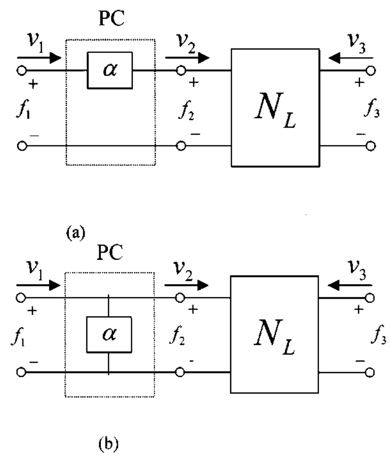

Fig. 4. (a) Series and (b) parallel PCs for two-port networks. A PC on only one of the ports is sufficient.

using (20)

$$\sum_{k=0}^{n} f_1(k)v_1(k) \geq 0 \qquad \forall n.$$

We may have an application in which the load applied to the one-port can be counted on to dissipate energy, for example, the load may be

$$f_1 = \beta(-v_1). \tag{23}$$

In this case, we may wish to replace zero on the right-hand side of (16) or (20) with a negative value such as

$$\hat{\beta} = \begin{cases} -\beta \displaystyle\sum_{k=0}^{n} v_1(k)^2, & \text{for impedance causality (16)} \\ -\dfrac{1}{\beta} \displaystyle\sum_{k=0}^{n} f_1(k)^2, & \text{for admittance causality (20).} \end{cases} \tag{24}$$

The PC design for the two-port network (Fig. 4) is a straightforward extension of (16)–(20). The PC for the two-port may be placed at either port.

When there are multiple elements (blocks) in a network (such as in Fig. 5), we can add a single PC to regulate energy production of the combined, open-ended system. In general, either velocity or force causality will be determined by the system architecture at the input port. As with the one-port, the causality determines whether a series or shunt PC is used. The PC should be placed at the input port in the selected configuration. Then, the system can be treated exactly as with the one-port element:

1) solve the network to obtain the output variable (force for impedance causality, velocity for admittance);
2) update the PO and compute the PC according to (16) or (20);
3) compute and return the modified output variable.

III. Potential Problems

We have described two implementations of the PC, the series (velocity conserving) and parallel (force conserving) controllers. In the next paragraph we suggest some performance

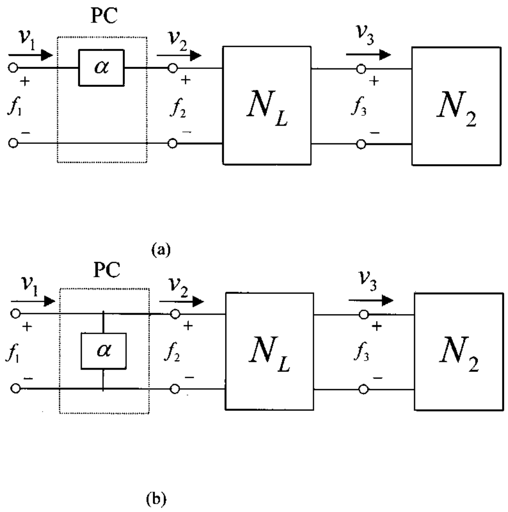

Fig. 5. (a) Series and (b) parallel PCs for network systems.

limitations and issues that arise in the series PC. The same issues arise in dual form in the parallel controller, but these will not be described in detail to save space.

A potential problem which may occur with the series PC is that the forces required to dissipate the generated energy may exceed the actuator limits. This is especially true if velocity happens to be small. A related problem is that, due to the well-known difficulties of computing a noise-free velocity signal, we might want to limit the value of α to avoid "magnifying noise." For these reasons, we may want to limit the magnitude of the force generated by the series PC, limit the maximum value of α, or both. In this case, the PC may not be able to dissipate all of the energy supplied by a subnetwork in one sample time. The excess energy must be stored in the system for the next sample time. We explore this issue in the experimental section below.

IV. Simulation Examples

In this section, we will illustrate the operation of the PO and PC with simulation of a simple virtual wall with impedance causality (velocity in, force out). Two separate simulations, one in Matlab/simulink, and one in a C program using trapezoidal integration, were used. The wall consists of a first-order, penalty-based, spring damper model (Fig. 6) executed at 1000 Hz. We can easily create active behavior of this system by setting the damping parameter, b, to a negative value. The wall generates forces only when $x(t) > 0$. In our simulation, the wall is probed by a point following a sinusoidal velocity trajectory [Fig. 7(a)]. With positive damping [$k = 710$ N/m, $b = 50$ Ns/m, Fig. 7(b)], the PO value increases with time although not monotonically. When the damping parameter is changed to a negative value [$b = -50$ Ns/m, Fig. 7(c)], the PO value returns after each "bounce" to a more negative value, indicating the active behavior of the environment. Finally, with $b = -50$ Ns/m and both PO and series PC [Fig. 7(d)], the value of the PO is constrained to be greater than zero and the amplitude of the bounces stays constant.

The second simulation is of a basic haptic interface system (Fig. 8) consisting of the human operator (HO), the haptic interface (HI), the PC, and the virtual environment (VE). Note

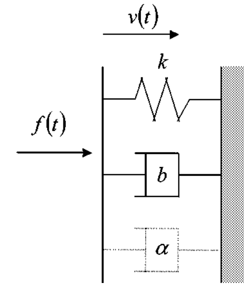

Fig. 6. Simple virtual wall model for simulation testing of PO/PC.

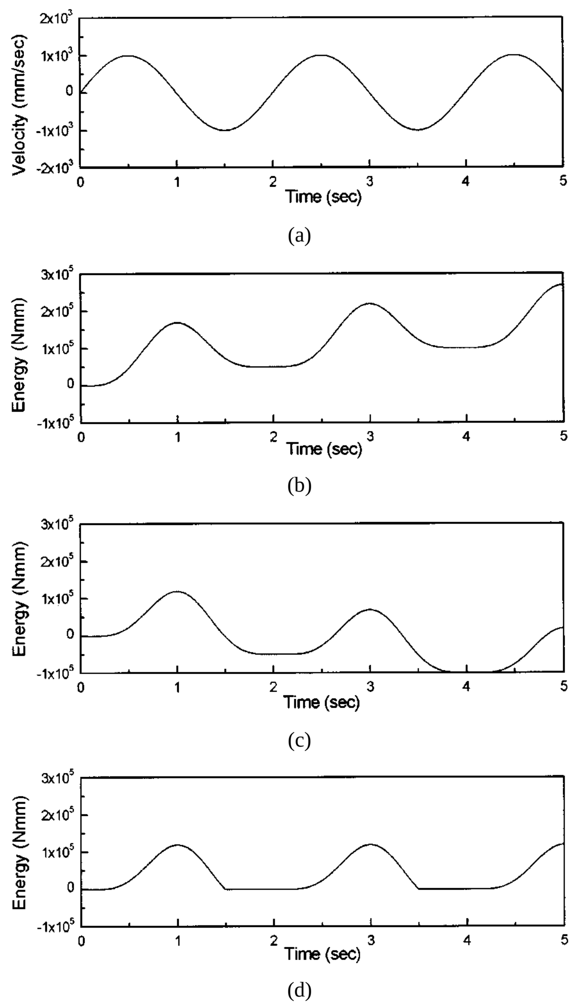

Fig. 7. Simulation response for simple virtual wall system. When driven by: (a) a sinusoidal velocity profile, (b) system dissipates energy when damping is positive and (c) generates energy when damping is negative. When wall damping is still negative and passivity controller is operating, (d) dissipation is constrained to be positive and the system is stable.

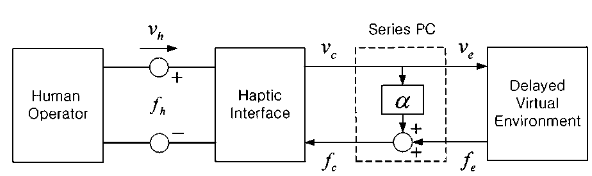

Fig. 8. More detailed simulation model of a complete haptic interface system and passivity controller. System blocks are (left to right) human operator, haptic interface, passivity controller (α), and virtual environment.

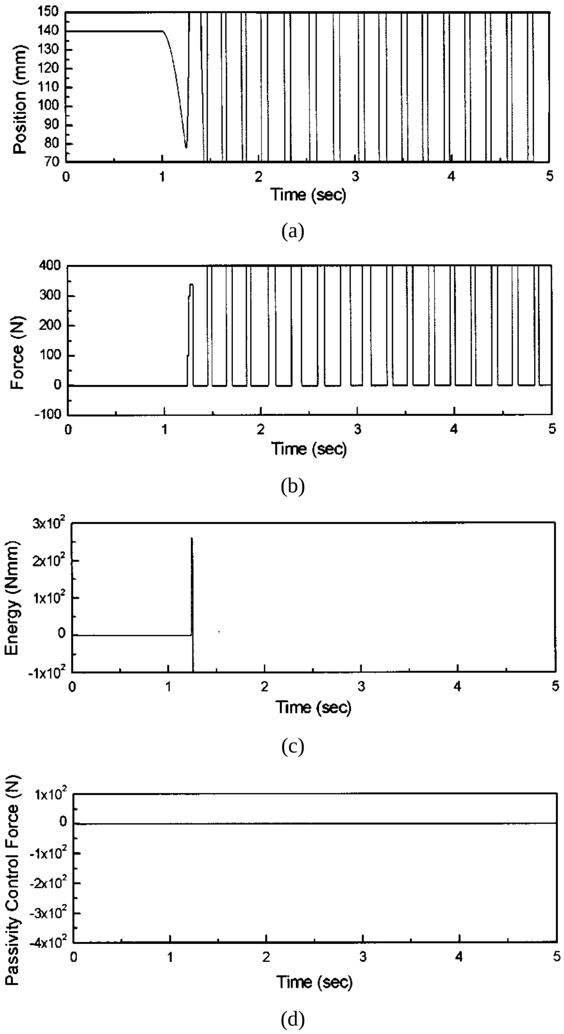

Fig. 9. Simulated response of haptic interface model (Fig. 8). Passivity controller is not operating (bottom trace) and system is unstable. (a) Position. (b) Force. (c) Energy. (d) Passivity control force.

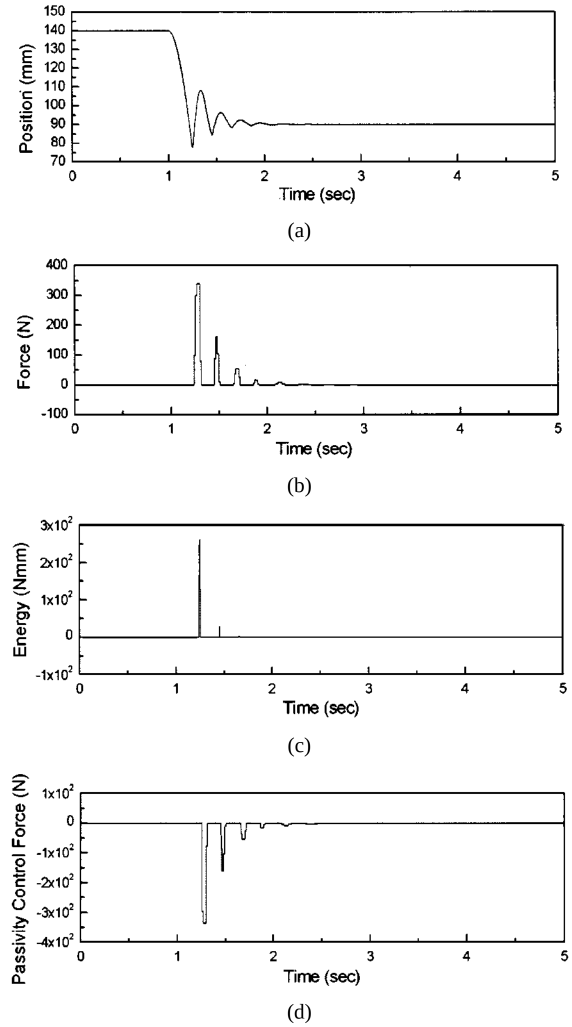

Fig. 10. Simulation of haptic interface system (Fig. 8) with passivity controller enabled. Passivity controller operates briefly (bottom trace) to damp out oscillations and constrain energy dissipation to be positive. (a) Position. (b) Force. (c) Energy. (d) Passivity control force.

that the series PC appears in Fig. 8 to be connected in parallel, but this is an artifact of switching to block diagram notation for the connections between the HI, PC, and VE. The VE includes a spring constant of 30 kN/m and operates at a relatively slow sampling rate of 66.67 Hz (15 ms). We set up the PO to monitor only the virtual environment and the PC. We also assume that the HI has a positive damping value, b. Thus, we do not want to control passivity to zero, but rather to a negative value

$$\alpha(n) = \begin{cases} \dfrac{\left(W(n) + b\sum\limits_{k=0}^{n} v_e(k)^2\right)}{v_e(n)^2}, & \\ \quad \text{if } W(n) < -b\sum\limits_{k=0}^{n} v_e(k)^2 & \\ 0, \qquad \text{if } W(n) \geq -b\sum\limits_{k=0}^{n} v_e(k)^2 & \end{cases} \tag{25}$$

where

$$W(n) = \sum_{k=0}^{n} f_e(k)v_e(k) + \sum_{k=0}^{n-1} \alpha(k)v_e(k)^2. \tag{26}$$

Without the PC, the system is highly unstable when driven to contact (Fig. 9). With the added PC, the system achieves stable contact after about 3 bounces (Fig. 10), which complete in about 0.5 s. Note however, that PC force is about 350 N for the first bounce.

V. Experiment

Finally, we implemented the PO and PC in our Excalibur three-axis, high force output, haptic interface system [15], [9] in the laboratory. This system consists of the following elements (Fig. 11): human operator (HO), haptic interface (HI), haptic controller (HC) having feedforward gravity compensation and friction compensation, the PC, and the virtual environment (VE). This system is entirely synchronous at 1000 Hz. The HI senses position in 0.1-mm increments, and can display up to 200 N force inside a 300 × 300 × 200-mm workspace. The force resolution is 0.096 N. The virtual environment consisted of virtual Lego-like blocks.

A. Contact With High Stiffness

In this experiment, the PO accounted for energy flow in the HC, PC, and VE. We also assumed significant dissipation in the

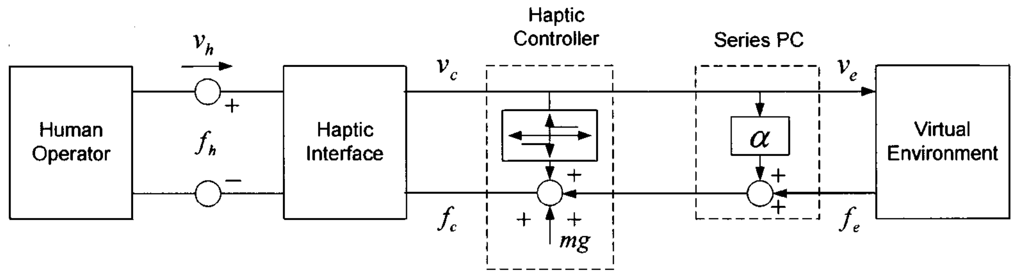

Fig. 11. Block diagram of experimental test system. An additional block (center) shows friction and gravity compensation elements.

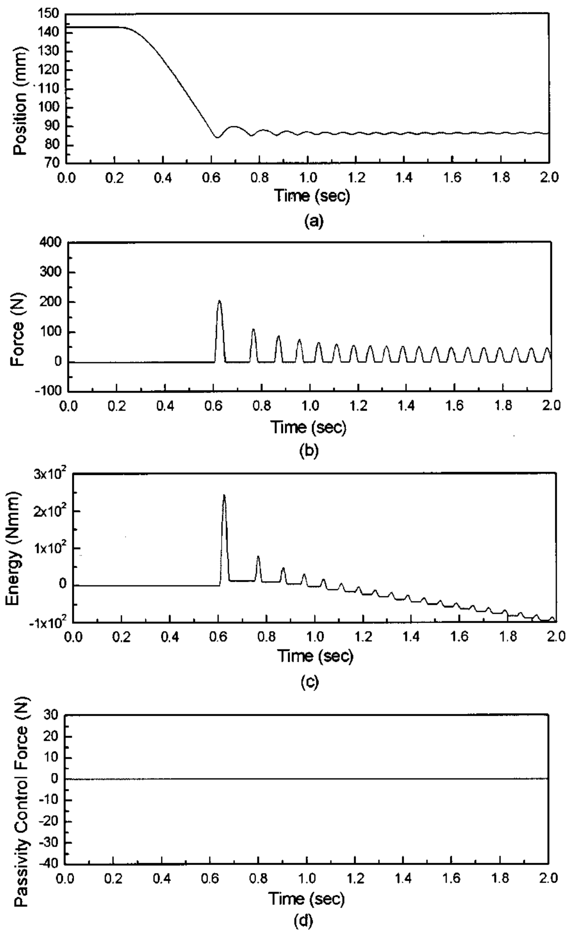

Fig. 12. Experimental results: contact with virtual environment (stiffness = 90 kN/m). Passivity controller is inactive and te system exhibits sustained contact oscillations. (a) Position. (b) Force. (c) Energy. (d) Passivity control force.

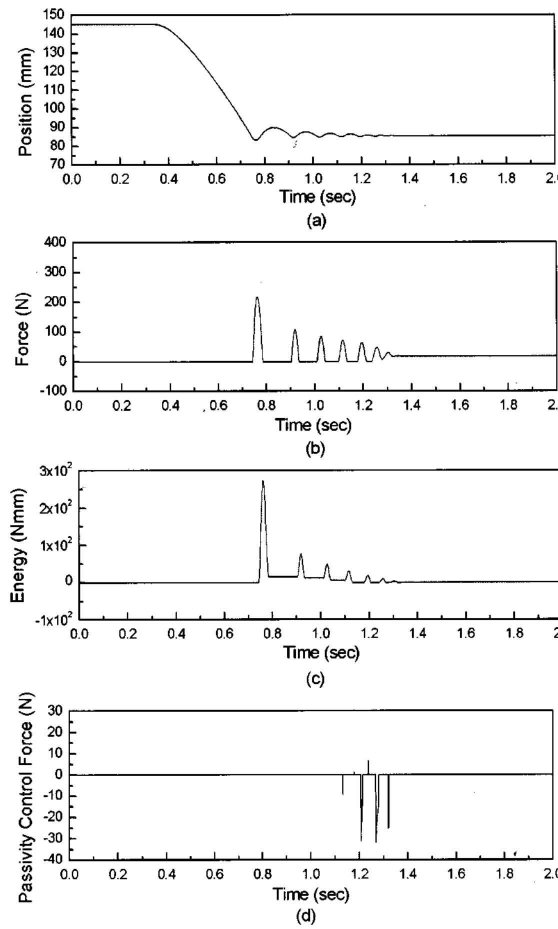

Fig. 13. Experimental results: contact with same virtual environment as in Fig. 12 with passivity controller operating. Oscillation is suppressed by brief pulses of force from the PC (bottom trace). Note that the initial "bounce" behaved passively, but subsequent smaller bounces were active. (a) Position. (b) Force. (c) Energy. (d) Passivity control force.

HO and HI ($b = 35$ Ns/m) and so used a nonzero threshold for the PC. In the first experiment, without the PC, the operator approached the virtual object ($k = 90$ kN/m) at about 200 mm/s [Fig. 12(a)]. Contact was unstable, resulting in an oscillation observable as force pulses [Fig. 12(b)], the value of the PO [Fig. 12(c)] was initially positive, but grew more and more negative with each contact. Interestingly, the initial bounce was passive, but the subsequent smaller bounces were active.

In the second experiment, with the PC turned on, the operator approached contact at the same velocity [Fig. 13(a)], but stable contact was achieved with about 6 bounces [Fig. 13(b)]. Again the first bounce can be seen to behave passively, but subsequent smaller bounces were active [Fig. 13(c)]. On the fourth bounce, the PC began to operate [Fig. 13(d)], and eliminated the oscillation. The PC force was less than 40 N, well within our actuator capabilities. However, in some cases PC force may add to other forces so we cannot tell from this alone whether or not actuator saturation occurred.

B. Control Force Limit

In the next experiment, we study the effect of limiting PC force to ± 20 N. The result is almost the same (Fig. 14) with some slightly longer pulses observed in the PC output [Fig. 14(d)] and some positive forces observed at the end of the PC output.

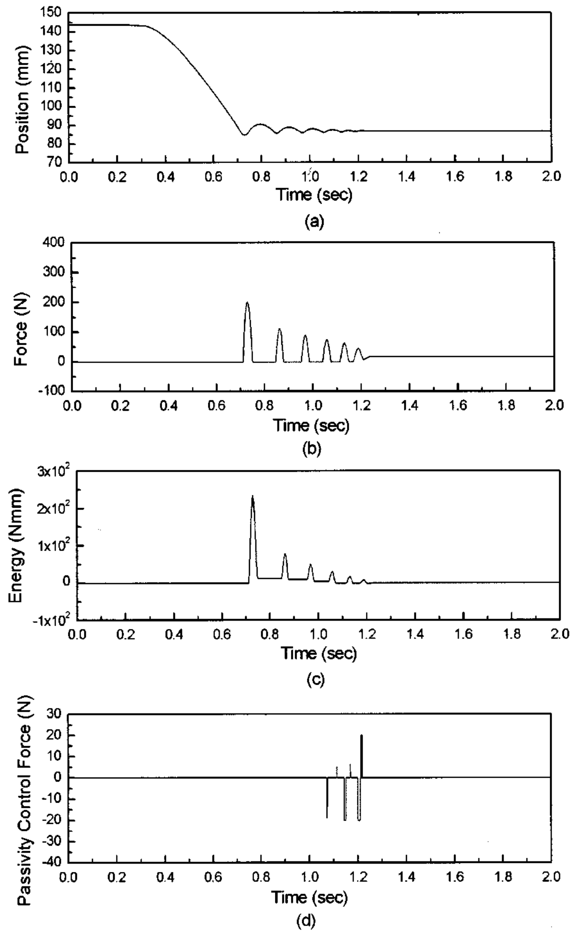

Fig. 14. Experimental results: same conditions as for Fig. 12, but the passivity controller force is limited to ±20 N. System is stable despite imposing a force limit to represent actuator saturation. (a) Position. (b) Force. (c) Energy. (d) Passivity control force.

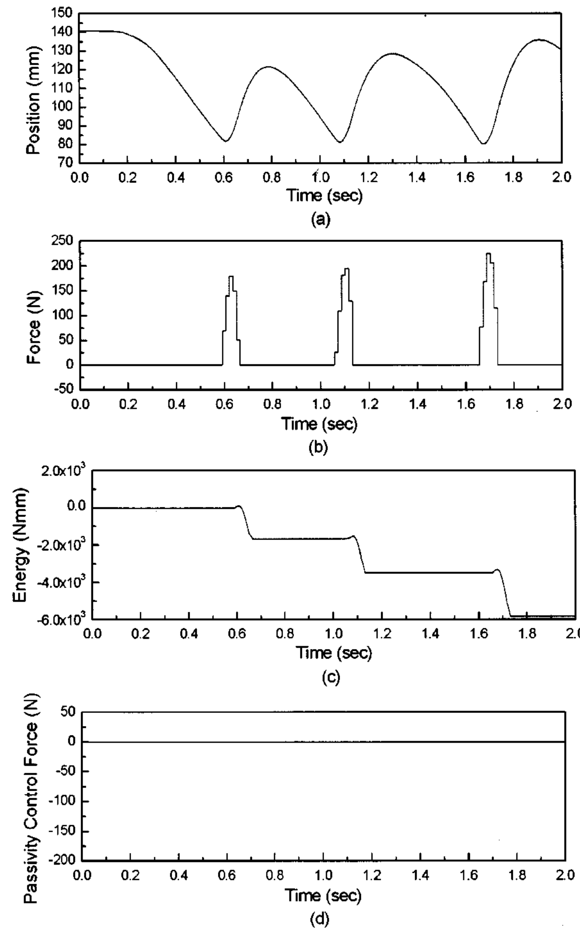

Fig. 15. Experimental results: stiffness reduced to 30 kN/m, but virtual environment slowed down to 67 Hz instead of 1000 Hz. Passivity controller is off and the system is highly unstable. (a) Position. (b) Force. (c) Energy. (d) Passivity control force.

C. Delayed Environment

One of the most challenging problems for further application of haptics is application to slow computing environments. These slow VEs are characteristic of complex simulations such as deformable objects for surgery or macro-molecular dynamics. We modified the basic Excalibur system to artificially slow down the VE to a rate of 66.67 Hz. The output force value of the simulation was held constant for 15 samples and then replaced with the new force value based on its input 15 samples prior. Environment stiffness was set to 30 kN/m.

Without PC, the result is a very unstable system (Fig. 15). The sampling delay due to the slow VE is visible in the shape of the force pulses which are as high as 200 N [Fig. 15(b)]. With PC, the contact was stabilized within a single bounce (Fig. 16). The contact force [Fig. 16(b)] is limited to a single pulse which tapers exponentially during about 1 s. The value of the PO [Fig. 16(c), note change in scale] consists of a single positive peak and is constrained to positive. The passivity control output [Fig. 16(d)] consists of a single large pulse, followed by a noise-like signal during the exponential decay of force ($t =$ 0.8 s to 1.2 s). The noisy behavior of the PC coincides with a period of low velocity [Fig. 16(a), $t =$ 0.8–1.2 s].

VI. Discussion

The haptic controller of the Excalibur system contains two features which are illustrated by our analysis. First, the controller compensates for gravity by adding a force in the positive Z direction equal to the weight of the Z-axis moving parts. This force component is constant and independent of the applied velocity, so it could be active or passive depending on the applied velocity. The gravity compensator will be passive over any closed trajectory in Z.

The second component is a Coulomb friction component

$$\begin{aligned} F_c(k) &= A\,\mathrm{sgn}(-v(k)), \qquad A>0\\ \sum_{k=0}^{n} F_c(k)v(k) &= A\sum_{k=0}^{n} v(k)\mathrm{sgn}(-v(k))\\ &= -A\sum_{n=1}^{k} |v(k)|\\ \sum_{k=0}^{n} F_c(k)v(k) &\le 0 \qquad \forall k. \end{aligned} \tag{27}$$

Clearly the Coulomb friction compensation term is active. Applying POs at several points around our Excalibur system

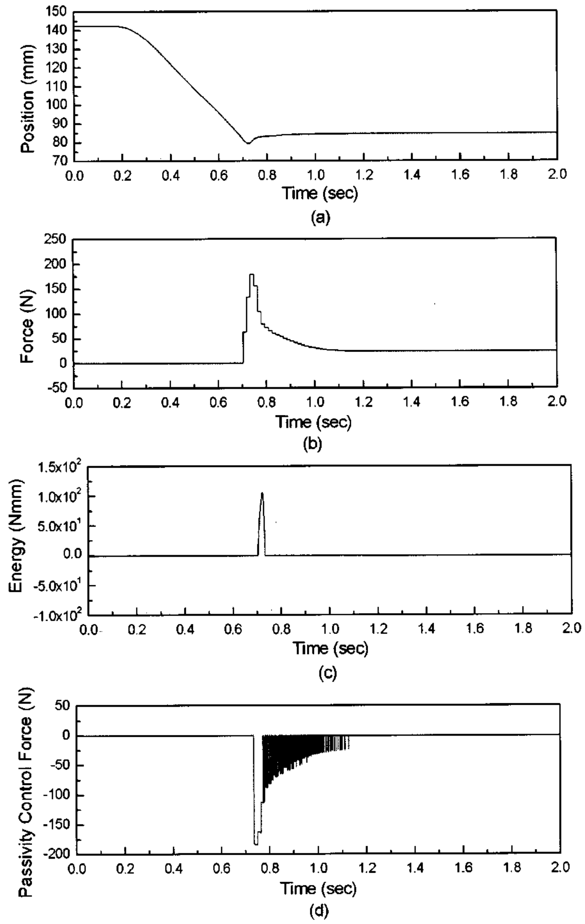

Fig. 16. Experimental results: same conditions as Fig. 15, but passivity controller is enabled. System now achieves stable, steady-state, contact. (a) Position. (b) Force. (c) Energy. (d) Passivity control force.

confirmed this analysis and showed that active behavior observed in Fig. 12 was primarily due to the friction compensation module.

The PC has several desirable properties for applications including haptic interface control. The PO and PC can both be implemented with simple software in existing haptic interface systems. The stability can be proven, yet it is not a fixed parameter design based on a worst case analysis. Thus, to maintain stability, the PC only degrades performance (through the added damping of the PC) when it is needed, and only in the amount needed.

Energy storage elements in the system do not have to be modeled, only dissipation. Dissipation in the elements outside the PO needs to be identified for optimum performance. However, the added performance due to modeling external dissipation [i.e., (24)] appears to be small. Thus, the PC can be very useful without any parameter estimation at all.

Nevertheless, the method has some limitations which we considered in advance or which become apparent in experimental testing. First, there are important cases in which virtual environments have very different behavior in different locations. Consider an environment which is very dissipative in location X and active in location Y. If the user spends a lot of time interacting at X, the PO may build up a large positive value. Then, if the user moves over and interacts with location Y, the PC will not operate until a corresponding amount of active behavior is observed. Theoretically, this is not a problem since even though the interaction may act unstable initially, the amount of instability will be bounded by the accumulated dissipation. Nevertheless, as a practical matter the amount of active behavior observed may exceed what is desired. One possibility we are exploring is "resetting" in which we derive heuristic rules for resetting the value of the PO to zero. These rules might, for example, detect a free motion state. However, such heuristics need to be experimentally tested in a wide variety of virtual environments.

Additional issues we described and tested were the performance of the system with limits imposed on the PC and sensitivity to low values of velocity. A patent application is pending on this technology.

VII. Future Work

In addition to resetting, there are several areas of future work which we will pursue. First, we identified issues associated with operation of the PC during periods of low velocity (series) or low force (parallel). We are studying a hybrid form of PC which includes both series and parallel dissipative elements and selects the most appropriate one for the operating conditions.

A second issue is the identification of the dissipation constant [β in (24)] for the human operator and haptic interface mechanism. We intend to study ways of automatically estimating this parameter during operation.

A third issue is sensitivity to noise in the velocity estimate used in the controller. This is evident in Fig. 16 when the velocity is near zero. Under these conditions, the user feels and hears some vibration for about one half second. Current work is studying a method for eliminating this phenomenon.

Finally, the benefits of the PO/PC may apply to other types of control systems such as motion control systems. We will study the possible applications of the PO/PC to increase the reliability and safety of this type of system.

Acknowledgment

The authors gratefully acknowledge M. Moreyra, R. Adams, and D. Klowden for the Excalibur system.

References

[1] J. E. Colgate, M. C. Stanley, and J. M. Brown, "Issues in the haptic display of tool use," in *Proc. IEEE/RSJ Int. Conf. on Intelligent Robotics and Systems*, Pittsburgh, PA, 1995, pp. 140–145.

[2] C. B. Zilles and J. K. Salisbury, "A constraint-based god-object method for haptic display," in *Proc. IEEE/RSJ Int. Conf. on Intelligent Robotics and Systems*, Pittsburgh, PA, 1995, pp. 146–151.

[3] R. J. Anderson and M. W. Spong, "Asymptotic stability for force reflecting teleoperators with time delay," *Int. J. Robot. Res.*, vol. 11, no. 2, pp. 135–149, 1992.

[4] G. Niemeyer and J. J. Slotine, "Stable adaptive teleoperation," *IEEE J. Ocean. Eng.*, vol. 16, pp. 152–162, 1991.

[5] J. E. Colgate and G. Schenkel, "Passivity of a class of sampled-data systems: Application to haptic interfaces," in *Proc. Amer. Control Conf.*, Baltimore, MD, 1994, pp. 3236–3240.

[6] N. Hogan, "Controlling impedance at the man/machine interface," in *Proc. IEEE Int. Conf. Robot. Automat.*, Scottsdale, AZ, 1989, pp. 1626–1631.

[7] H. M. Paynter, *Analysis and Design of Engineering Systems*. Cambridge, MA: MIT Press, 1961.

[8] B. Hannaford, "A design framework for teleoperators with kinesthetic feedback," *IEEE Trans. Robot. Automat.*, vol. 5, pp. 426–434, Aug. 1989.

[9] R. J. Adams and B. Hannaford, "Stable haptic interaction with virtual environments," *IEEE Trans. Robot. Automat.*, vol. 15, pp. 465–474, June 1999a.

[10] B. E. Miller, J. E. Colgate, and R. A. Freeman, "Passive implementation for a class of static nonlinear environments in haptic display," in *Proc. IEEE Int. Conf. Robot. Automat.*, Detroit, MI, May 1999a, pp. 2937–2942.

[11] ——, "Computational delay and free node environment design for haptic display," *Proc. ASME Dyn. Syst. Cont. Div.*, 1999b.

[12] ——, "Environment delay in haptic systems," in *Proc. IEEE Int. Conf. Robot. Automat.*, San Francisco, CA, April 2000, pp. 2434–2439.

[13] B. Gillespie and M. Cutkosky, "Stable user-specific rendering of the virtual wall," in *Proc. ASME Int. Mechanical Engineering Conf. Expo.*, vol. DSC-58, Atlanta, GA, Nov. 17–22, 1996, pp. 397–406.

[14] Y. Yokokohji, T. Imaida, and T. Yoshikawa, "Bilateral control with energy balance monitoring under time-varying communication delay," in *Proc. IEEE Int. Conf. Robot. Automat.*, San Francisco, CA, April 2000, pp. 2684–2689.

[15] R. J. Adams, D. Klowden, and B. Hannaford, "Stable haptic interaction using the Excalibur Force Display," in *Proc. IEEE Int. Conf. Robot. Automat.*, San Francisco, CA, 2000, pp. 770–775.

[16] R. J. Adams and B. Hannaford, "Excalibur, a three-axis force display," in *ASME Winter Annu. Meeting Haptics Symp.*, Nashville, TN, Nov. 1999b.

[17] C. A. Desoer and M. Vidyasagar, *Feedback Systems: Input–Output Properties*. New York: Academic, 1975.

[18] A. J. van der Schaft, *L2-Gain and Passivity Techniques in Nonlinear Control*, ser. Communications and Control Engineering Series. New York: Springer, 2000.

[19] J. C. Willems, "Dissipative dynamical systems—Part I: General theory," *Arch. Rat. Mech. An.*, vol. 45, pp. 321–351, 1972.

[20] L. O. Chua, C. A. Desoer, and E. S. Kuh, *Linear and Nonlinear Circuits*. New York: McGraw-Hill, 1987.

Blake Hannaford (S'82–M'84–SM'01) received the B.S. degree in engineering and applied science from Yale University, New Haven, CT, in 1977 and the M.S. and Ph.D. degrees in electrical engineering from the University of California, Berkeley, in 1982 and 1985, respectively.

Before beginning his graduate work, he held engineering positions in digital hardware and software design, office automation, and medical image processing. At Berkeley he pursued thesis research in multiple target tracking in medical images and the control of time-optimal voluntary human movement. From 1986 to 1989, he worked on the remote control of robot manipulators in the Man–Machine Systems Group in the Automated Systems Section of the NASA Jet Propulsion Laboratory, California Institute of Technology, Pasadena. He supervised that group from 1988 to 1989. Since September 1989, he has been at the University of Washington, Seattle, where he has been Professor of Electrical Engineering since 1997 and served as Associate Chair for Education from 1999 to 2001. His currently active interests include haptic displays on the Internet, and surgical biomechanics. He is the founding editor of *Haptics-e, The Electronic Journal of Haptics Research*.

Prof. Hannaford was awarded the National Science Foundation's Presidential Young Investigator Award and the Early Career Achievement Award from the IEEE Engineering in Medicine and Biology Society.

Jee-Hwan Ryu received the B.S. degree in mechanical engineering from Inha University, Inchon, Korea, in 1995, and the M.S. degree in mechanical engineering from Korea Advanced Institute of Science and Technology, Taejon, Korea, in 1995, where he is currently pursuing the Ph.D. degree in stable control of teleoperator and haptic interfaces.

In 1998, he worked as a visiting graduate student in the Bio-Robotics Division of Mechanical Engineering Laboratory, Japan, and he worked as a Visiting Scholar in the Biorobotics Laboratory in the Department of Electrical Engineering, University of Washington, Seattle, from April to July in 2000. His research interests include haptic displays and robust control.